Analytical and Bioanalytical Chemistry
https://doi.org/10.1007/s00216-022-04400-0

RESEARCH PAPER

Engineering an Ag/Au bimetallic nanoparticle-based acetylcholinesterase SERS biosensor for in situ sensitive detection of organophosphorus pesticide residues in food

Shuling Xu[1] · Min Li[1] · Xia Li[1] · Yanhui Jiang[2] · Linlin Yu[2] · Yue Zhao[2] · Liyuan Wen[3] · Qingwang Xue[1]

Received: 24 August 2022 / Revised: 6 October 2022 / Accepted: 21 October 2022

Abstract
Developing simple, efficient, and inexpensive method for trace amount organophosphorus pesticides' (OPs) detection with high sensitivity and specificity is of significant importance for guaranteeing food safety. Herein, an Ag/Au bimetallic nanoparticle-based acetylcholinesterase (AChE) surface-enhanced Raman scattering (SERS) biosensor was constructed for in situ simple and sensitive detection of pesticide residues in food. The principle of this biosensor exploited 4-mercaptophenylboronic acid (4-MPBA)-modified Ag/Au bimetallic nanoprobes as SERS signal probe to improve sensitivity and stability. The combination of AChE and choline oxidase (CHO) can hydrolyze acetylcholine (ATCh) to generate H_2O_2. The product of H_2O_2 selectively oxidizes the boronate ester of 4-MPBA, decreasing the Raman intensity of the B-O symmetric stretching. In the presence of OPs, it could inhibit the production of H_2O_2 by destroying the AChE activity, so the reduction of the SERS signal was also alleviated. Based on the principle, an Ag/Au bimetallic nanoparticle-based AChE SERS sensor was established without any complicated pretreatments. Benefiting from the synergistic effects of Ag/Au bimetallic hybrids, a linear detection range from 5×10^{-9} to 5×10^{-4} M was achieved with a limit of detection down to 1.7×10^{-9} M using parathion-methyl (PM) as the representative model of OPs. Moreover, the SERS biosensor uses readily available reagents and is simple to implement. Importantly, the proposed SERS biosensor was used to quantitatively analyze OP residues in apple peels. The levels of OPs detected in real samples by this method were consistent with those obtained using gas chromatography–mass spectrometry (GC–MS), suggesting the proposed assay has great potential applications for OPs in situ detection in food safety fields.

Keywords Acetylcholinesterase · Ag/Au bimetallic hybrids · In situ SERS biosensor · Organophosphorus pesticides

Introduction

Organophosphorus pesticides (OPs) have been extensively used in agriculture to protect crops from pests and insects for many years. However, OPs are well-known to inhibit the enzymatic activity of AChE, resulting in the accumulation of the neurotransmitter ATCh in the body, which can lead to fatal consequences to human central nervous system [1–5]. Therefore, the demand for detection of OP residues in rapid and sensitive method has urgently increased to guarantee food security. Traditional detection methods such as gas chromatography (GC) [6], liquid chromatography (LC) [7], high-performance liquid chromatography (HPLC), and mass spectrometry (MS) [8] have been utilized for the determination of OP residues. Although these techniques are capable of selectively detecting OPs, the complex processes and professional operation limit their practical applications. To address this critical issue, novel analysis techniques such as electrochemical analysis and [9] colorimetric [10] and fluorescent assay [11] have been developed. For example, Velusamy et al. fabricated an electrochemical sensor based on cellulose microfiber-supported reduced graphene oxide, which was successfully applied for

✉ Liyuan Wen
liyuanwen@163.com

✉ Qingwang Xue
xueqingwang1983@163.com

[1] School of Chemistry and Chemical Engineering, Liaocheng University, Liaocheng 252059, Shandong, China

[2] Center for Disease Control and Prevention of Liaocheng, Liaocheng, Shandong, China

[3] Earthquake Monitoring Center Station of Liaocheng, Earthquake Administration of Shandong Province, Liaocheng, Shandong, China

Published online: 04 November 2022

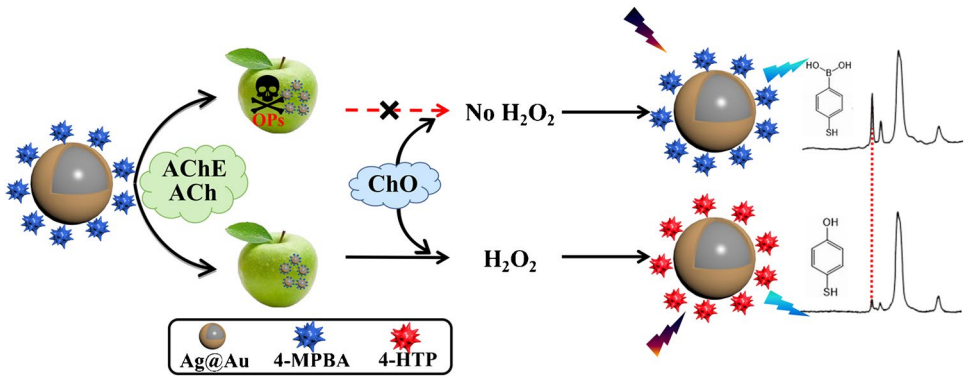

Scheme 1 Schematic illustration of an Ag/Au bimetallic nanoparticle-based acetylcholinesterase SERS biosensor for in situ sensitive detection of organophosphorus pesticide residues in food

the detection of fenitrothion in different water samples [12]. Yu et al. established a universal method for the measurement of chlorpyrifos in vegetables with modification-free C-dots as the fluorescent probes [13]. For the past few years, the SERS-based analytical technique has attracted extensive investigative attention in recent years, owing to its noninvasive, nonlabeling, fingerprint-type detection capability, as well as ultrahigh sensitivity [14–17].

It is generally accepted that SERS provides significant amplification of Raman signals for analytes close to plasmonic metal, because of the localized surface plasmonic resonances (LSPRs) effect [18–20]. Noble metal nanoparticles (NPs) are commonly used as SERS-active materials due to their excellent plasmonic properties. As one of the most excellent candidates for SERS application, Ag NPs can support LSPRs right across the visible spectrum; however, its low resistance to oxidation is a draw-back for sustained SERS performance in the long term [21, 22]. While Au-based SERS substrates are more stable, the cost is much higher than that of Ag-based counterparts. It is noteworthy that Ag/Au bimetallic hybrids could achieve enhanced SERS performance and stability through synergistic effects of the Ag and Au on nanoscale [23–25]. For instance, Fortuni et al. reported an Au-coated Ag NP substrates for SERS detection, the thin Au layer provides oxidation resistivity while maintaining the broad spectral range SERS sensitivity of Ag NPs [26]. Gao et al. synthesized alloyed Ag/Au nanospheres that combined the extinction cross-section and high stability, showing a superior Raman signal intensity [27].

In recent decades, the SERS technology plays a major role in the analysis of pesticide residues, numerous SERS substrates with large Raman enhancement ability have been constructed [28–30]. As it is reported, conventional SERS substrates based on silicon or glass templates cannot be attached to irregular food surfaces, thereby making in situ surface Raman analysis impossible. In these regards, transparent and flexible SERS substrates can be used for in situ analysis by swabbing or wrapping onto food surfaces which have gained considerable attention [31–33]. However, the flexible SERS substrates constructed by depositing Ag or Au NPs onto flexible frameworks are either tedious in the preparation or low efficiency in performance, thereby inhibiting their practical applications [34]. Recently, bienzyme-based biosensors based on AChE/ChOx strategy are evolving into a promising technology for the sensitive detection of OPs, ChOx is a limiting enzyme in this bienzyme system, and the characteristics of choline enzymatic oxidation affect the specificity of the measurements [35, 36]. OPs can destroy the activity of AChE and inhibit the production of H_2O_2, which can be effectively determined by electrochemical, colorimetric, and fluorescence biosensors, and thus, low-level detection of OP residues in agricultural has been realized [37–41]. Inspired by the efficiency and convenience of SERS technology, we conclude that the SERS biosensor based on the selectively oxidation effect between H_2O_2 and nanoprobe would provide a powerful candidate for in situ detection of OPs.

In this work, we report an SERS biosensor based on the bienzyme AChE/ChOx for in situ detection of OPs on apple peels. The proposed sensing strategy includes two sequential reactions:

$$\mathrm{ACh} + \mathrm{H_2O} \xrightarrow{\mathrm{AChE}} \mathrm{Choline} \quad (1)$$

$$\mathrm{Choline} + \mathrm{O_2} \xrightarrow{\mathrm{ChOx}} \mathrm{H_2O_2} + \mathrm{betaine} \quad (2)$$

The hydrolysis of ACh was catalyzed by AChE to form choline (1), and then the oxidation of choline in the presence of ChOx generates betaine and H_2O_2 (2). As shown in Scheme 1, the Ag/Au NPs modified by 4-MPBA (Ag/Au NPs-MPBA) were developed as SERS nanoprobe. The reaction of ATCh with AChE to form choline that is in turn catalytically oxidized by ChOx to produce H_2O_2 which can oxidize 4-MPBA to 4-mercaptophenol (4-MP) and SERS signal changed accordingly [42]. OPs can destroy the activity of AChE and inhibit the production of H_2O_2;

thus, the SERS signal change of 4-MPBA subsequently weakened. According to the relationship that the SERS signal of 4-MPBA in response to the increase of OPs, a SERS biosensor for in situ detection of OPs on apple peels was established.

Experimental

Chemicals

All chemicals were of analytical grade and used without further purification. Silver nitrate ($AgNO_3$), gold chloride trihydrate ($HAuCl_4{\cdot}3H_2O$), ammonium hydroxide ($NH_3{\cdot}H_2O$), trisodium citrate dehydrate, L-ascorbic acid (AA), and hydrogen peroxide (H_2O_2) (30%) were obtained from Sinopharm Chemical Reagent Co., Ltd. 4-Mercaptophenylboronic acid (4-MPBA), acetylcholinesterase (AChE), choline oxidase (ChO), and acetylthiocholine (ATCh) iodide were purchased from Macklin Biochemical Co., Ltd. Parathion-methyl (PM) standards were obtained from Liaocheng Center for Disease Control and Prevention. The fruits were bought from a local supermarket. The Milli-Q water (18.2 MΩ·cm) or ethanol was used for the preparation of the samples.

Instrumentation

Transmission electron microscopy (TEM) images were taken on a transmission electron microscope (JEM-2100, JEOL) operated at 200 kV. Scanning electron microscopy (SEM) images and energy-dispersive X-ray spectroscopy (EDS) mapping were taken on a field emission scanning electron microscope (Helios G4 CX, Thermo Scientific) with acceleration voltage of 15 and 10 kV, respectively. Dynamic light scattering (DLS) data were obtained using Zeta Nanosizer (Malvern). Ultraviolet–visible (UV–Vis) absorption spectra were recorded by a UV-3600 PC spectrophotometer. The gas chromatography–mass spectrometry (GC–MS) measurements were performed on a TSQ8000EVO spectrometer (Thermo Fisher Scientific Co.). SERS experiments were conducted using a Renishaw InVia Reflex confocal microscope equipped with a 50× objective and 633 nm as the excitation wavelength. The output power of the laser was 5 mW, and the collection time was 10 s.

Synthesis of Ag/Au NPs-MPBA nanoprobes

To synthesize Ag/Au NPs, 1 mL of trisodium citrate (0.1 M) and 2 mL of AA (0.2 mM) were added to 5 mL of water (the pH of the pure water was adjusted to 9.0 by $NH_3{\cdot}H_2O$). Next, 2.5 mL of $AgNO_3$ (0.1 M) solution was injected stepwise into the mixture under stirring. The solution color changed to reddish brown within <30 s, indicating the formation of Ag NPs. After another 2 min of stirring, 100 μL of $HAuCl_4$ (30 mM) was added to the mixture; the color of the mixture changed from brownish to grayish green, indicating the formation of Ag/Au NPs. Next, the obtained Ag/Au NPs were washed and centrifuged three times and diluted in 1 mL of phosphate-buffered solution (PBS, 10 mM, pH =7.4) for further experiment. Finally, 100 μL of 4-MPBA ethanol solution (10 μM) was added to 1 mL of Ag/Au NPs' colloidal solution for 12 h at room temperature and then centrifuged at a speed of 10000r for 10 min. After that, the precipitate was dispersed with 1 mL of PBS; the achieved Ag/Au NPs-MPBA nanoprobes were stored at 4 °C before use. The modification of 4-MPBA molecules on the Ag NPs was the same procedure as the Ag/Au NPs-MPBA nanoprobe preparation.

SERS measurement of H_2O_2

First, 30% H_2O_2 was diluted with pure water for different concentrations. For H_2O_2 detection, 50 μL of H_2O_2 solution with various concentrations was added to 500 μL of Ag/Au NPs-MPBA colloidal solution and mixed well. After being incubated for 30 min, 50 μL of the mixed solution was dropped onto a glass slide and dried naturally for SERS measurements.

SERS determination of OPs

For OP detection, PM was selected as the models. The stock solutions of PM (10^{-3} M) were prepared freshly in ethanol and then diluted to the final concentration before use. The measurements for PM were carried out as follows: 50 μL of OP solution with different concentrations were mixed with 500 μL of Ag/Au NPs-MPBA colloidal solution containing AChE (3 U/mL), ATCh (100 μm), and ChOx (1 U/mL) to prepare the AChE-OPs-ATCh-CHOx solution. After incubating for 30 min, 50 μL of the mixed solution was dropped onto a glass slide and dried naturally for SERS measurements.

Determination of OPs in real samples

Apple peels were washed with deionized water and ethanol before use and then cut into 0.5 × 0.5 cm^2. Fifty μL of PM solution with different concentrations were spread on the peels and dried naturally in air. For in situ SERS detection, 50 microliter of Ag/Au NPs-MPBA colloidal solution containing AChE (3 U/mL), ATCh (100 μm), and ChOx (1 U/mL) was carefully dropped on the apple peels; the SERS spectra were recorded after the droplet drying (about 50 min). Furthermore, the obtained results were consistent with that of GC–MS, suggesting the potential applicability of the proposed assay for PM detection in real samples.

Results and discussion

Characterization of Ag/Au NPs

Ag/Au NPs have been prepared by the addition of $HAuCl_4$ into colloidal solution of the synthesized Ag NPs; the morphology, particle size distribution information, and UV−vis spectra of Ag NPs were shown in Fig. S1. The SEM and TEM images of the Ag/Au NPs in Fig. 1A and B indicated the synthesized Ag/Au NPs are almost homogeneous spherical shape. The SEM images at different magnifications and the corresponding EDS maps were shown in Fig. S2. The average diameter of the Ag/Au NPs is about 28 nm (Fig. 1C), which is larger than that of Ag NPS (Fig. S1B). For the pure Ag NPs, the maximum localized surface plasmon resonance (LSPR) position was located at 420 nm (Fig. S1C); as the Au was deposited on the Ag NPs, the LSPR position displayed a red shift to 440 nm (Fig. 1D, black line), confirming the successful formation of bimetallic Ag/Au NPs [43]. After functionalizing the Ag/Au NPs with 4-MPBA, a new absorption peak located at 252 nm was observed (Fig. 1D, red line), which attributed to the characteristic peak of 4-MPBA [44].

The SERS spectrum of Ag/Au NPs-MPBA nanoprobe and the ordinary Raman spectrum of solid 4-MPBA were compared in Fig. S3. It was shown that the two Raman bands for Ag/Au NPs-MPBA nanoprobes at 993 and 1011 cm^{-1} attributed to the B–O symmetric stretching and the deformation of B–O–H on boric acid group of 4-MPBA. The other two peaks at 1071 and 1562 cm^{-1} were assigned to C–H in-plane deformation and C–C stretching vibrations on the benzene ring [45]. The results indicated that 4-MPBA was successfully conjugated with Ag/Au NPs. The SERS spectra of the Ag/Au NPs were investigated after storage for 1 month to test the stability of the nanoprobe. In contrast to the Ag NPs, no obvious decrease in the intensity of SERS peaks for 4-MPBA was observed (Fig. S4), suggesting the obtained Ag/Au NPs-MPBA nanoprobes may be kept in storage for a long time.

Mechanism of SERS biosensor

This sensing strategy involves the reaction of ATCh with AChE to form choline that is in turn catalytically oxidized by ChOx to produce H_2O_2, which have specific effect on 4-MPBA to form 4-MP, leaving SERS signal intensity reduce of the B−O symmetric stretching at 993 cm^{-1}. In the presence of OPs, the activity of AChE would be inhibited, and the enzyme-generated H_2O_2 decrease, which weakened the reduction of B−O symmetric stretching at 993 cm^{-1}, as shown in Scheme 1. In addition, the SERS intensity of the C−H in-plane deformation at 1071cm^{-1} did not change, which could be used as an internal standard to realize quantitative detection of OPs based on the ratiometric peak intensity of I_{1071}/I_{993}. Scheme 1 represents the mechanism for in situ detection of OPs using the prepared

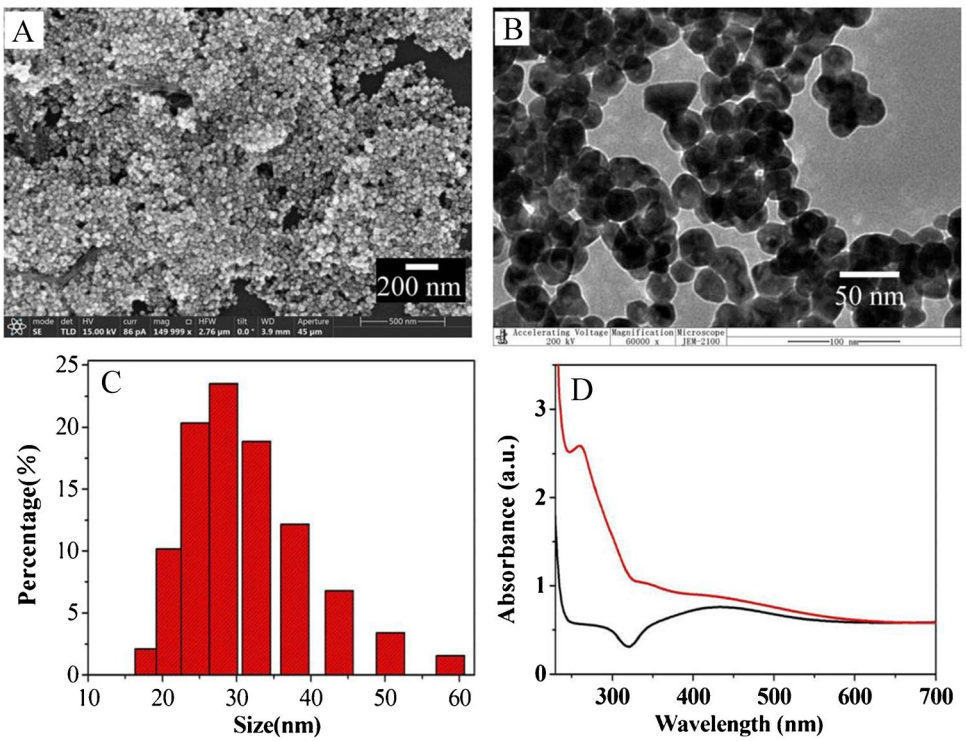

Fig. 1 **A** SEM and **B** TEM image of the Ag/Au NPs. **C** Particle size distribution curve of the Ag/Au NPs. **D** UV−Vis spectra of the Ag/Au NPs (black line) and Ag/Au NPs-MPBA (red line)

SERS biosensor based on AChE-inhibited assay. When the Ag/Au NPs-MPBA nanoprobes were individually incubated with ATCh, ChOx, and AChE or PM under the same conditions, almost no change was observed in SERS spectra of 4-MPBA (Fig. S5A–D). While Ag/Au NPs-MPBA nanoprobes were incubated with AChE-ATCh-CHOx solution, the SERS intensity of B−O peaks decreased due to the specific effect of H_2O_2 on B−O symmetric stretching of 4-MPBA (Fig. S5E).

The SERS spectra of the Ag/Au NPs-MPBA nanoprobes treated with different concentrations of H_2O_2 were investigated. As shown in Fig. S6A, the intensity ratio of I_{1071}/I_{993} increased linearly with the logarithm of H_2O_2 within the range from 10^{-6} to 10^{-3} M. The linear equation can be described as $Y = 1.8X + 19.2$, and the correlation coefficient R^2 was as high as 0.988, as shown in Fig. S6B.

Optimization of the detection conditions

To effectively detect OPs, the related parameters including the incubation time, pH value of the reaction system, and the concentrations of the reactant were optimized. The time-dependent SERS spectra of Ag/Au NPs-MPBA nanoprobes in the AChE-ATCh-CHOx solution were investigated. As shown in Fig. 2A, the intensity ratio of I_{1071}/I_{993} sustained a stable value when the incubation time reached 30 min, indicating that the reaction between H_2O_2 and 4-MPBA has been completed within 30 min. The intensity ratio of I_{1071}/I_{993} of Ag/Au NPs-MPBA changed under different pH conditions; the intensity reached a maximum when the pH is in the range of 7.0−8.0 (Fig. 2B). Therefore, 30-min reaction time and PBS of pH =7.4 were considered in the further experiments.

Moreover, it is important to optimize the concentrations of AChE and ChOx, because they have an effect on the generated H_2O_2 and consequently affect SERS intensity of Ag/Au NPs-MPBA nanoprobes. The SERS spectra of Ag/Au NPs-MPBA incubated with different ratios of AChE/ChOx for 30 min were shown in Fig. S7. The results indicated that the SERS intensity of the B−O symmetric stretching at 993 cm^{-1} decreased with the increasing of ATCh concentration. Depending on the ratio of AChE/ChOx, the magnitude of the decrease was different. As shown in Fig. 3, the intensity ratio of I_{1071}/I_{993} showed linearity with the ATCh concentration from 0 to 100 μM, which could be expressed as (A) $Y = 0.046X + 1.542$, (B) $Y = 0.056X + 1.384$, and (C) $Y = 0.059X + 1.521$,

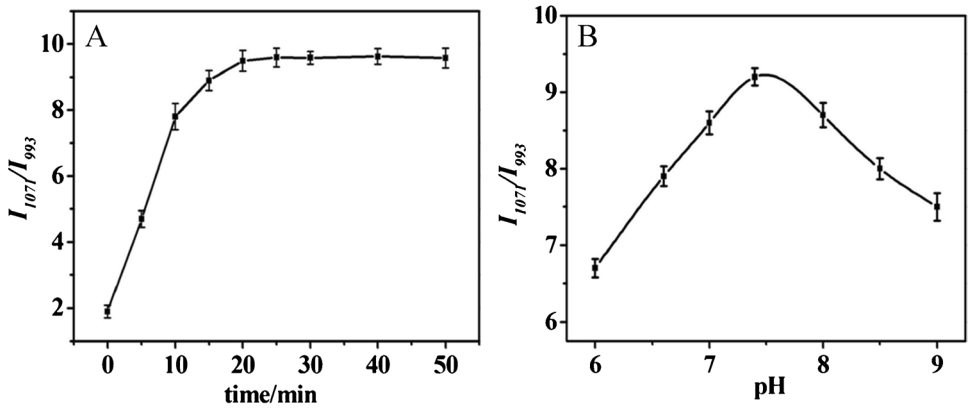

Fig. 2 Optimization of the reaction time (**A**) and pH value (**B**) of the AChE-inhibited strategy. The AChE, ChOx, and PM concentrations were 3 U/mL, 1 U/mL, and 10^{-5} M, respectively

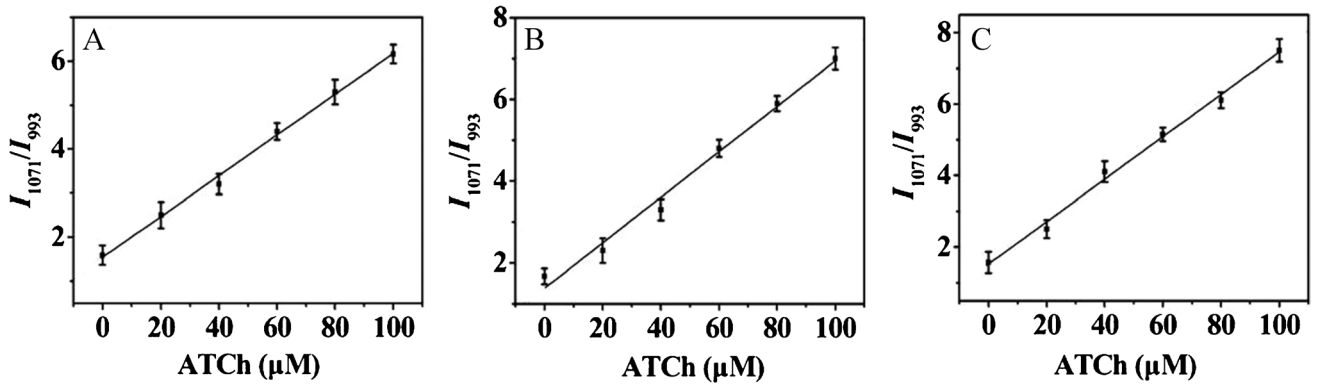

Fig. 3 Curve of ratiometric SERS signal I_{1071}/I_{993} value versus the ATCh concentrations from 0 to 100 μM. The concentrations of AChE and ChOx were 1 U/mL and 3 U/mL (**A**), 1 U/mL and 1 U/mL (**B**), 3 U/mL and 1 U/mL (**C**), respectively

respectively. The absolute value of the slope of the (C) line was greater than the other two, which indicated that the highest effect was reached when the concentrations of AChE and ChOx were 3 U/mL and 1U/mL.

SERS detection of OPs

To investigate the performances of the prepared SERS biosensor for the detection of OPs, we investigated PM as the representative model OPs. Under optimal conditions, PM with different concentrations was introduced to Ag/Au NPs-MPBA-AChE-ATCh-CHOx mixture, respectively. Figure 4A depicted the SERS spectra of Ag/Au NPs-MPBA nanoprobes for PM concentrations from 5×10^{-9} to 5×10^{-4} M. PM can inhibit the activity of AChE and reduce the generation of H_2O_2. The SERS signal changes of B−O symmetric stretching at 993 cm^{-1} were weakened upon increasing PM. As can be noticed in Fig. 4B, the intensity ratio of I_{1071}/I_{993} decreased almost linearly with the logarithm of PM concentration. The linear regression equation was $Y = -1.4X - 3.0$, with a correlation coefficient of R^2=0.982. The limit of detection (LOD) was calculated as 1.7×10^{-9} M which is determined based on 3σ/K (σ is the standard deviation of the blank, and K is the calibration of the curve). When the concentration was converted to the molar to area ratio (m/a), the LOD of PM was 2.2×10^{-9} mol/m^2 (for calculation details, see "concentration conversion" part of the Supporting Information).

The comparison between the SERS biosensor and other reported methods for the detection of PM was presented in Table S1. The results indicated that the proposed AChE-inhibited SERS sensor exhibited sensitivity to OPs compared with other reported methods. This excellent performance should be attributed to the synergistic effects of bimetallic hybrids, improving the SERS property of Ag/Au NPs-MPBA nanoprobe. Moreover, SERS biosensor does not require sample pretreatment and is a simple, rapid, and cost-efficient way for in situ detection of actual samples.

Anti-interference ability of the SERS biosensor for the detection of OPs

It is essential to estimate the anti-interference capability of the SERS biosensor from the possible interference species in analytes. PM (10^{-6} M) and some other existing species, including Ca^{2+}, Mg^{2+}, Na^{+}, Zn^{2+}, Fe^{3+}, vitamin C (VC), glucose, fructose, tannic acid, cysteine, glycine, asparagic acid (Asp), and tartaric acid (10^{-4} M) were introduced to Ag/Au NPs-MPBA-AChE-ATCh-CHOx solution under the above experimental conditions. As shown in Fig. 5, it can be observed that when the above-mentioned species was alone in the reaction system, the SERS signal of the Ag/Au NPs-MPBA nanoprobe changed very little. All these results vividly indicated that the proposed bienzyme-based SERS biosensor possessed excellent anti-interference ability for the detection of OPs in practical applications.

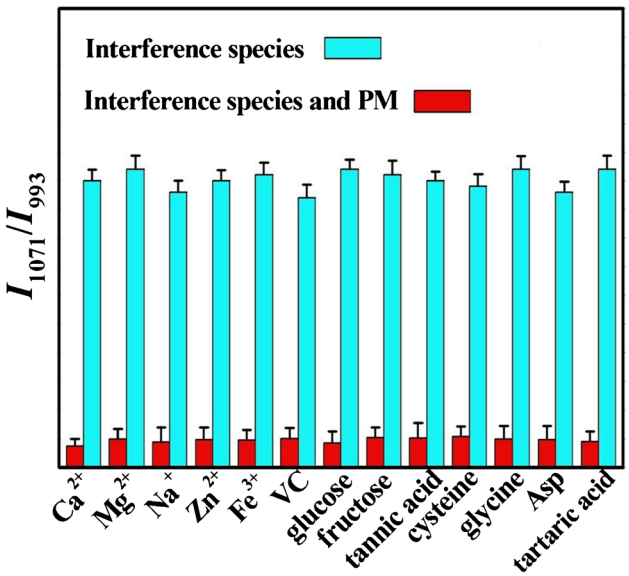

Fig. 5 The inhibition efficiency of the SERS biosensor with the possible interference species on the apple peels

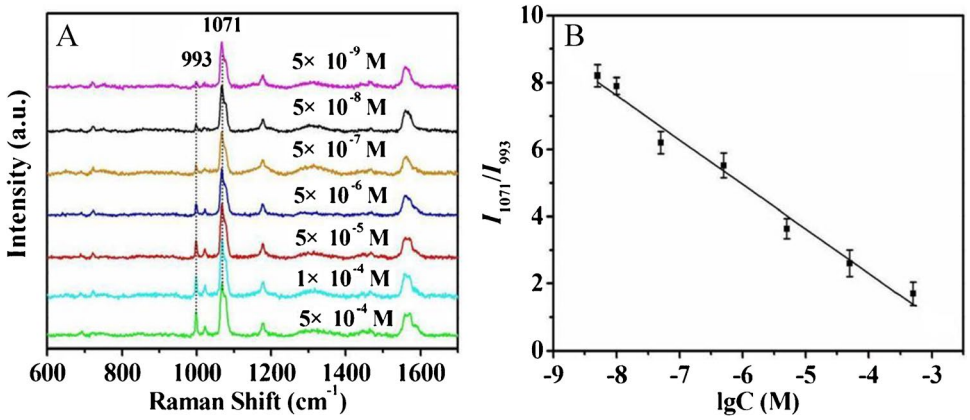

Fig. 4 **A** SERS spectra of Ag/Au NPs-MPBA at different concentrations of PM from 5×10^{-9} to 5×10^{-4} M. **B** Plot of the ratiometric SERS signal value of I_{1071}/I_{993} vs. the logarithmic concentration of PM

Table 1 Comparison between the results obtained from SERS and GC–MS assay for PM in apple peels

Sample	Spiked value (μmol/m^2)	Measured value (μmol/m^2)		Recovery (%)	
		SERS	GC–MS	SERS	GC–MS
1	20	18.8	21.5	94	107
2	40	38.2	39.1	95	97
3	60	65.8	59.1	109	98
4	80	78.6	83.7	98	104
5	100	91.9	106.3	92	106

Real sample analysis

To demonstrate the in situ detection of OP residues on fruit surface, an apple was firstly washed with ultrapure water and ethanol carefully. Fifty microliter of the prepared PM solution with different concentrations was sprayed onto the apple peels. After the evaporation of the solvent, 50 μL of the Ag/Au NPs-MPBA-AChE-ATCh-CHOx solution was dropped onto the apple peels and incubated for 30 min. Finally, SERS signals were collected in situ from the apple peels. The digital photograph of in situ detection of PM on the apple peels using the proposed AChE-inhibited assay and the SERS spectra of the apple peels without PM spraying were shown in Fig. S8. To test the accuracy of the SERS biosensor, the PM concentrations in apple peels were also detected by GC–MS as shown in Table 1. The results obtained by using this assay coincided well with those obtained by using GC–MS, indicating that the proposed SERS biosensor can be successfully applied for detecting OPs in real samples. Therefore, it was possible to use the proposed SERS biosensor to detect OPs in real samples.

Conclusion

In summary, a novel SERS biosensor based on an AChE-inhibited assay for the detection of OPs residues was developed. The SERS spectra of Ag/Au NPs-MPBA nanoprobe could be changed by H_2O_2, which is produced by the enzyme-catalyzed reaction of AChE. OP residues can effectively inhibit the activity of AChE and decrease the production of H_2O_2. Based on this principle, the quantitative detection of OPs was carried out, and the results showed wide linear range and high sensitivity. Compared with other methods for pesticide residue, the proposed SERS biosensor was quite simple in operation and especially suitable for in situ detection. These advantages make the assay has great application prospects in food safety and the real-time monitoring of agricultural production.

Supplementary Information The online version contains supplementary material available at https://doi.org/10.1007/s00216-022-04400-0.

Acknowledgements We thank the Natural Science Foundation of China (21675072), the Natural Science Foundation of Shandong Province (ZR2019MB068, ZR2022MB012), the Project of Shandong Province Higher Educational Science and Technology Program (KJ2018BZC043), and the Young Innovative Talents Introduction and Cultivation Program for Colleges and Universities of Shandong Province: Innovative Research Team on biomedical sensing and food safety Research.

Declarations

Conflict of interest The authors declare no competing interests.

References

1. Liu T, Xu SR, Lu SY, Qin P, Bi B, Ding HD, Liu Y, Guo XC, Liu XH. A review on removal of organophosphorus pesticides in constructed wetland: performance, mechanism and influencing factors. Sci Total Environ. 2019;651:2247–68.
2. Han W, Tian Y, Shen X. Human exposure to neonicotinoid insecticides and the evaluation of their potential toxicity: an overview. Chemosphere. 2018;192:59–65.
3. Guo YR, Liu R, Liu Y, Xiang DD, Liu YH, Gui WJ, Li MY, Zhu GN. A non-competitive surface plasmon resonance immunosensor for rapid detection of triazophos residue in environmental and agricultural samples. Sci Total Environ. 2018;613:783–91.
4. Cao J, Wang M, Yu H, She Y, Cao Z, Ye J, Abd El-Aty AM, Hacimuftuoglu A, Wang J, Lao S. An overview on the mechanisms and applications of enzyme inhibition-based methods for determination of organophosphate and carbamate pesticides. J Agric Food Chem. 2020;68:7298–315.
5. Jokanovic M. Neurotoxic effects of organophosphorus pesticides and possible association with neurodegenerative diseases in man: a review. Toxicology. 2018;410:125–31.
6. Zhou T, Xiao X, Li G. Microwave accelerated selective Soxhlet extraction for the determination of organophosphorus and carbamate pesticides in ginseng with gas chromatography/mass spectrometry. Anal Chem. 2012;84:5816–22.
7. Deme P, Azmeera T, Kanjilal S, Jonnalagadda P, Upadhyayula VS. LC-MS/MS determination of organophosphorus pesticide residues in coconut water. Food Anal Methods. 2013;6:1162–9.
8. Zhu F, Ruan W, He M, Zeng F, Luan T, Tong Y, Lu T, Ouyang G. Application of solid-phase microextraction for the determination of organophosphorus pesticides in textiles by gas chromatography with mass spectrometry. Anal Chim Acta. 2009;650:202–6.
9. Pang S, Yang T, He L. Review of surface enhanced Raman spectroscopic (SERS) detection of synthetic chemical pesticides. TrAC, Trends Anal Chem. 2016;85:73–82.
10. Cai Y, Zhu H, Zhou W, Qiu Z, Chen C, Qileng A, Li K, Liu Y. Capsulation of AuNCs with AIE effect into metal−organic framework for the marriage of a fluorescence and colorimetric biosensor to detect organophosphorus pesticides. Anal Chem. 2021;93:7275–82.
11. Shen Y, Yan F, Huang X, Zhang X, Zhang Y, Zhang C, Jin J, Li H, Yao S. A new water-soluble and colorimetric fluorescent probe for highly sensitive detection of organophosphorus pesticides. RSC Adv. 2016;6:88096–103.
12. Velusamy V, Palanisamy S, Chen SW, Balu S, Yang TCK, Banks CE. Novel electrochemical synthesis of cellulose microfiber entrapped reduced graphene oxide: a sensitive electrochemical assay

for detection of fenitrothion organophosphorus pesticide. Talanta. 2019;192:471–7.
13. Lin B, Yan Y, Guo M, Cao Y, Yu Y, Zhang T, Huang Y, Wu D. Modification-free carbon dots as turn-on fluorescence probe for detection of organophosphorus pesticides. Food Chem. 2018;245:1176–82.
14. Li H, Lv W, Yang Q, Li Q, Li F. Inorganic Recognizer-Assisted Homogeneous electrochemiluminescence determination of organophosphorus pesticides via target-controlled emitter release. J Agric Food Chem. 2021;69:6087–95.
15. Fu G, Sun DW, Pu H, Wei Q. Fabrication of gold nanorods for SERS detection of thiabendazole in apple. Talanta. 2019;195:841–9.
16. Zhang Y, Wang Z, Wu L, Pei Y, Chen P, Cui Y. Rapid simultaneous detection of multi-pesticide residues on apple using SERS technique. Analyst. 2014;139:5148–54.
17. Xu ML, Gao Y, Han XX, Zhao B. Detection of pesticide residues in food using surface-enhanced Raman spectroscopy: a review. J Agric Food Chem. 2017;65:6719–26.
18. Zhang Z, Yu Q, Li H, Mustapha A, Lin M. Standing gold nanorod arrays as reproducible SERS substrates for measurement of pesticides in apple juice and vegetables. J Food Sci. 2015;80:450–8.
19. Qian K, Yang L, Li Z, Liu J. A new-type dynamic SERS method for ultrasensitive detection. J Raman Spectrosc. 2013;44:21–8.
20. Liu Z, Wang Y, Deng R, Yang L, Yu S, Xu S, Xu W. Fe_3O_4 @ Graphene Oxide@Ag particles for surface magnet solid-phase extraction surface-enhanced Raman scattering (SMSPE-SERS): from sample pretreatment to detection all-in-one. ACS Appl Mater Interfaces. 2016;8:14160–8.
21. Yan J, Han XJ, He JJ, Kang LL, Zhang B, Du YC, Zhao HT, Dong CK, Wang H-L, Xu P. Highly sensitive surface-enhanced Raman spectroscopy (SERS) platforms based on silver nanostructures fabricated on polyaniline membrane surfaces. ACS Appl Mater Interfaces. 2012;4:2752–6.
22. Zhang X-Y, Hu A, Zhang T, Lei W, Xue X-J, Zhou Y, Duley WW. Self-assembly of large-scale and ultrathin silver nanoplate films with tunable plasmon resonance properties. ACS Nano. 2011;5:9082–92.
23. Liu Z, Cheng L, Zhang L, Jing C, Shi X, Yang Z, Long Y, Fang J. Large-area fabrication of highly reproducible surface enhanced Raman substrate via a facile double sided tape-assisted transfer approach using hollow Au−Ag alloy Nanourchins. Nanoscale. 2014;6:2567–72.
24. Liu BH, Han GM, Zhang ZP, Liu RY, Jiang CL, Wang SH, Han MY. Shell thickness-dependent Raman enhancement for rapid identification and detection of pesticide residues at fruit peels. Anal Chem. 2012;84:255–61.
25. Zheng X, Chen Y, Chen Y, Bi N, Qi H, Qin M, Song D, Zhang H, Tian Y. High performance Au/Ag core/shell bipyramids for determination of thiram based on surface-enhanced Raman scattering. J Raman Spectrosc. 2012;43:1374–80.
26. Fortuni B, Inose T, Uezono S, Toyouchi S, Umemoto K, Sekine S, Fujita Y, Ricci M, Lu G, Masuhara A, Hutchison JA, Latterini L, Uji-i H. Chem Commun. 2017;53:11298–301.
27. Gao CB, Hu YX, Wang MS, Chi MF, Yin YD. Fully alloyed Ag/Au nanospheres: combining the plasmonic property of Ag with the stability of Au. JAm Chem Soc. 2014;136:7474–9.
28. Zhang Z, Yu Q, Li H, Mustapha A, Lin M. Standing gold nanorod arrays as reproducible SERS substrates for measurement of pesticides in apple juice and vegetables. J Food Sci. 2015;80:450–8.
29. Alsammarraie FK, Lin M. Using standing gold nanorod arrays as surface-enhanced Raman spectroscopy (SERS) substrates for detection of carbaryl residues in fruit juice and milk. J Agric Food Chem. 2017;65:666–74.
30. Liu X, Osada M, Kitamura K, Nagata T, Si D. Ferroelectric-assisted gold nanoparticles array for centimeter-scale highly reproducible SERS substrates. Sci Rep. 2017;7:1–8.
31. Li S, Pang C, Ma X, Zhang Y, Xu Z, Li J, Zhang M, Wang M. Microfluidic paper-based chip for parathion-methyl detection based on a double catalytic amplification strategy. Microchim Acta. 2021;188:438–45.
32. Xia D, Jiang P, Cai Z, Zhou R, Tu B, Gao N, Chang G, He H, He Y. Ag nanocubes monolayer-modified PDMS as flexible SERS substrates for pesticides sensing. Microchim Acta. 2022;189:232–41.
33. Cui H, Li S, Deng S, Chen H, Wang C. Flexible, transparent, and free-standing silicon nanowire SERS platform for in situ food inspection. ACS Sens. 2017;2:386–93.
34. Liou P, Nayigiziki FX, Kong F, Mustapha A, Lin M. Cellulose nanofibers coated with silver nanoparticles as a SERS platform for detection of pesticides in apples. Carbohydr Polym. 2017;157:643–50.
35. Hua X, Liu X, Shi H, Wang Y, Kim HJ, Gee SJ, Wang M, Liu F, Hammock BD. Development of a heterologous enzymelinked immunosorbent assay for organophosphorus pesticides with phage-borne peptide. RSC Adv. 2014;4:42445–53.
36. Tvorynska S, Barek J, Josypčuk B. Acetylcholinesterase-choline oxidase-based mini-reactors coupled with silver solid amalgam electrode for amperometric detection of acetylcholine in flow injection analysis. J Electroanal Chem. 2022;860:113883–92.
37. Yi Y, Zhu G, Liu C, Huang Y, Zhang Y, Li H, Zhao J, Yao S. A label-free silicon quantum dots-based photoluminescence sensor for ultrasensitive detection of pesticides. Anal Chem. 2013;85:11464–70.
38. Yan X, Song Y, Zhu CZ, Li HX, Du D, Su XG, Lin YH. MnO_2 nanosheet-carbon dots sensing platform for sensitive detection of organophosphorus pesticides. Anal Chem. 2018;90:2618–24.
39. Huang S, Yao J, Chu X, Liu Y, Xiao Q, Zhang Y. One-Step Facile synthesis of nitrogen-doped carbon dots: a ratiometric fluorescent probe for evaluation of acetylcholinesterase activity and detection of organophosphorus pesticides in tap water and food. J Agric Food Chem. 2019;67:11244–55.
40. Han Y, Ye Z, Wang F, Chen T, Wei L, Chen L, Xiao L. Single-particle enumeration-based ultrasensitive enzyme activity quantification with fluorescent polymer nanoparticles. Nanoscale. 2019;11:14793–801.
41. Zheng Q, Yu Y, Fan K, Ji F, Wu J, Ying Y. A nano-silver enzyme electrode for organophosphorus pesticide detection. Anal Bioanal Chem. 2016;408:5819–27.
42. Cheng W, Tang P, He X, Xing X, Xing M, Lu L, Ju P, Wang Y, Liu S, Lu X, Zhong L. Dynamic monitoring and quantitative characterization of intracellular H_2O_2 content by using SERS based boric acid nanoprobe. Talanta. 2020;214:120863–70.
43. Zhang X, Zhang G, Zhang B, Su Z. Synthesis of hollow Ag–Au bimetallic nanoparticles in polyelectrolyte multilayers. Langmuir. 2013;29:6722–7.
44. Cheng W, Tang P, He X, Xing X, Xing M, Lu L, Ju P, Wang Y, Liu S, Lu X, Zhong L. Dynamic monitoring and quantitative characterization of intracellular H_2O_2 content by using SERS based boric acid nanoprobe. Talanta. 2020;214:120863–70.
45. Li X, Duan X, Yang P, Li L, Tang B. Accurate in situ monitoring of mitochondrial H_2O_2 by robust SERS nanoprobes with a Au−Se interface. Anal Chem. 2021;93:4059–65.